Article

Effects of In-Process Temperatures and Blending Polymers on Acrylonitrile Butadiene Styrene Blends

Muhammad Harris [1,2,*], Johan Potgieter [1], Hammad Mohsin [3], Karnika De Silva [4] and Marie-Joo Le Guen [5]

[1] Massey Agrifood Digital Lab, Massey University, Palmerston North 4410, New Zealand; j.potgieter@massey.ac.nz

[2] Department of Industrial and Manufacturing Engineering, Rachna College of Engineering and Technology, Gujranwala 52250, Pakistan

[3] Department of Polymer Engineering, National Textile University, Faisalabad 37610, Pakistan; mhammad@ntu.edu.pk

[4] Faculty of Engineering, The University of Auckland, Auckland 1023, New Zealand; k.desilva@auckland.ac.nz

[5] Scion, Rotorua 3046, New Zealand; mariejoo.leguen@scionresearch.com

* Correspondence: m.harris@massey.ac.nz or engr.harris@.uet.edu.pk

Abstract: Acrylonitrile butadiene styrene (ABS) is a renowned commodity polymer for additive manufacturing, particularly fused deposition modelling (FDM). The recent large-scale applications of 3D-printed ABS require stable mechanical properties than ever needed. However, thermochemical scission of butadiene bonds is one of the contemporary challenges affecting the overall ABS stability. In this regard, literature reports melt-blending of ABS with different polymers with high thermal resistance. However, the comparison for the effects of different polymers on tensile strength of 3D-printed ABS blends was not yet reported. Furthermore, the cumulative studies comprising both blended polymers and in-process thermal variables for FDM were not yet presented as well. This research, for the first time, presents the statistical comparison of tensile properties for the added polymers and in-process thermal variables (printing temperature and build surface temperature). The research presents Fourier transform infrared spectroscopy (FTIR) and thermogravimetric analysis (TGA) to explain the thermochemical reasons behind achieved mechanical properties. Overall, ABS blend with PP shows high tensile strength (≈31 MPa) at different combinations of in-process parameters. Furthermore, some commonalities among both blends are noted, i.e., the tensile strength improves with increase of surface (bed) and printing temperature.

Keywords: fused deposition modelling; polypropylene; high density polyethylene; additive manufacturing; blending

1. Introduction

Acrylonitrile butadiene styrene (ABS) is one of the two commercially known polymers (ABS and PLA) for additive manufacturing (AM) [1–3]. In fused deposition modelling (FDM), ABS is the oldest elastomeric (rubbery) thermoplastics [4]. It is known for good mechanical strength [5], hydrophobicity [6], and chemically inertness [7]. These properties are caused due to a copolymeric structure of ABS [8]. Acrylonitrile butadiene styrene (ABS) is rubbery polymer constituted of two phases, i.e., styrene-acrylonitrile (SAN) and butadiene (PD) [9]. The composition of each of two phases ascertain a specific set of characteristics. For example, the continuous amorphous phase of styrene-acrylonitrile (SAN) results in stability to stress cracking, heat-based structural damages, and chemical effects [9]. The polybutadiene (PB) phase causes high toughness [10]. Along with benefits, the noted disadvantage of high composition of butadiene is the oxidation due to the action of inorganic acids or thermal degradation. The double bond (Pi bond) scission in butadiene causes the ABS copolymer to degrade [11]. Additionally, ABS also reports

degradation in mechanical characteristics due to the environmental temperatures above 40 °C [12].

One of the suitable processing methods to overcome degradation of double bonds of polybutadiene (PB) is melt blending of ABS with different polymers [12,13]. Generally, two types of approaches are adopted regarding melt blending. i.e., chemical compatibilization and physical interlocking [14]. In this regard, the chemical compatibilization results in comparative better mechanical properties [14]. For example, Angel et al. [15] reports significant effects of compatibilizer (Styrene-ethylene-butylene-styrene, SEBS) on binary and ternary blends of ABS. The authors present increase of ductility in binary blend (ABS:SEBS) with the increase of SEBS contents from 5% to 20%. However, the overall tensile strength of compatibilized blends (binary and ternary) are less than neat PLA printed in horizontal orientation. Carmen et al. [16] reports the ternary blend of ABS, ultra-high molecular weight polyethylene (UHMWPE), and SEBS. The compatibilized blend achieves increase in elongation (5.7% to 8.4%) with decrease of UHMWPE percentage. However, the overall tensile strength (24 MPa) of ternary blend system was less than neat ABS (34 MPa). Siyuan et al. [17] introduces the first ever compatibilized blend of ABS with polymethylmethacrylate (PMMA) and methacrylate–butadiene–styrene (MBS). The blend system reports comparatively better tensile properties (41 MPa) as compared to that of neat PLA (39.4 MPa) [17].

The abovementioned literature proves that chemical compatibilization is not a unanimous solution for improving the overall tensile strength as compared to neat polymer. The literature also highlights the effects of different polymers on overall properties of ABS blends. Therefore, this highlights a need to explore an alternative processing approach to develop polymer blends with uniform mechanical properties.

Concerning alternative processing approach, the authors of this research have developed a novel approach of partial chemical grafting and high physical interlocking in their recent work [18,19]. In this regard, the blends of ABS with high density polyethylene (HDPE) and polypropylene (PP) are recently presented [18,19]. Both blends report the increase of thermal stability [18,19]. The reason for high thermal stability is overwhelming physical interlocking that avoids the degradation of double bonds of SAN [18,19]. However, both articles do not provide any comparative analysis for the effects of two different polymer additives (HDPE and PP). Furthermore, the effects of in-process temperatures (bed and printing) on the tensile properties are still not traced comparatively for HDPE and PP.

The objective of this research is to analyse the effects of different polymer additives and in-process temperatures (bed and printing) on a partially compatibilized blend with overwhelming physical interlocking. The research reports two blend of ABS:HDPE:PE-g-MAH and ABS:PP:PE-g-MA with overwhelming physical interlocking. In this regard, the research utilizes a mixed level full factorial ANOVA analysis to design the design of experiments (DoE) for three variables, i.e., build surface temperature, printing temperature, and polymer additives. The chemical analysis techniques of Fourier transform infrared spectroscopy (FTIR), and thermogravimetric analysis (TGA) are used to analyse the reasons for mechanical results.

2. Materials and Methods

2.1. Materials

Neat acrylonitrile butadiene styrene (PA-747) of Polylac, Distrupol was purchased from TCL Hunt New Zealand. The melt flow index (MFI) of PA747 ABS is 13 g/10 min at 220 °C. Polypropylene of Dowlex, Dow Inc. was purchased from TCL Hunt, New Zealand. The melt flow index of Dowlex PP is 10 g/10 min. High density polyethylene (IP-10) of Dowlex, Dow Inc. was obtained from TCL Hunt, New Zealand. The melt flow index of Dowlex HDPE is 10 g/10 min. Polyethylene graft maleic anhydride (A8525) of Shenzhen

Jindaquan Technology Co. Ltd. was procured from China. The Composition of polyethylene and maleic anhydride in PE-g-MAH is 95:5 by weight percentage.

2.2. Polymer Melt Blending

All polymers were dried at 40 °C in an oven for 6 h at Scion, New Zealand. The ABS pellets were separately mixed with PP and HDPE with constant composition of PE-g-MAH. The two compositions were blended in single screw extruder (HAAKE™) at Scion, New Zealand. The mixing compositions for two blends are provided in Table 1. The temperature from feeder to nozzle were set for 10 heating zones, i.e., 170 °C, 170 °C, 175 °C, 175 °C, 175 °C, 175 °C, 175 °C, 175 °C, 165 °C and 145 °C. Each temperature zone had an accuracy of ±3 °C. Furthermore, the single screw extruder was operated at a feed rate of 20 rpm and speed of 200 rpm. The blend was pelletized in cylindrical shapes pellets with an approximate length of 1.5 mm.

Table 1. Compositions prepared in single screw extruder.

| Composition | Polymers Weight Percentage | | | |
	ABS	HDPE	PP	PE-g-MAH
1	48	48		4
	48		48	4
2	92	7.5		0.5
	92		7.5	0.5

2.3. Design of Experiment

The experiments were designed using a mixed level general full factorial ANOVA. Three variables were used for design of experiments: (1) printing (nozzle) temperature, (2) surface (bed) temperature, and (3) polymer. Printing (nozzle) temperature was designed with three levels, i.e., 180 °C, 190 °C, 200 °C. Surface (bed) temperature consists of three levels, i.e., 30 °C, 50 °C, 70 °C. The factor "polymer" was designed with two material which were designated as two levels, i.e., HDPE and PP. The experiments were randomised and analysed with a confidence level of 95%. The confidence level of 95% will statistically analyse the 5% chance of the deterioration in tensile strength due to the beforementioned three variables. The selected value (95%) for confidence level was taken from literature [20–22]. The DoE is provided in Table 2.

The 3D printing was performed on an in-house built pellet 3D printer [23]. The pellet printer was selected to avoid the thermal variations that are expected to appear in the raw blends due to the thermal shearing process of filament making [12,24]. Furthermore, the pellet 3D printer has a liquid cooling system that maintains the thermochemical properties of the raw blend proficiently until 3D printing as compared to that of filament 3D printer [23].

Table 2. Mixed level general full factorial design of experiments with randomization.

StdOrder	RunOrder	PtType	Blocks	Printing Temperature (°C)	Build Surface Temperature (°C)	Polymer
3	1	1	1	180	50	HDPE
10	2	1	1	190	50	PP
2	3	1	1	180	30	PP
15	4	1	1	200	50	HDPE
6	5	1	1	180	70	PP
17	6	1	1	200	70	HDPE
9	7	1	1	190	50	HDPE
14	8	1	1	200	30	PP

5	9	1	1	180	70	HDPE
16	10	1	1	200	50	PP
12	11	1	1	190	70	PP
7	12	1	1	190	30	HDPE
1	13	1	1	180	30	HDPE
13	14	1	1	200	30	HDPE
4	15	1	1	180	50	PP
8	16	1	1	190	30	PP
11	17	1	1	190	70	HDPE
18	18	1	1	200	70	PP

2.4. 3D Printing

3D printing was performed on a custom-made pellet 3D printer [23] as shown in Figure 1. Pellet 3D printer was selected to avoid thermal degradation of raw material in process of filament extrusion (melt blending) [24].

The CAD drawings of ASTM D638 Type IV [25] was designed on Solidworks version 2018 and saved in standard tessellation language (stl.) format. The dimensions are shown in Figure 2. The "stl" files were sliced into layers using a slicing software (Slic3er). The parameters for slicing are given in Table 3.
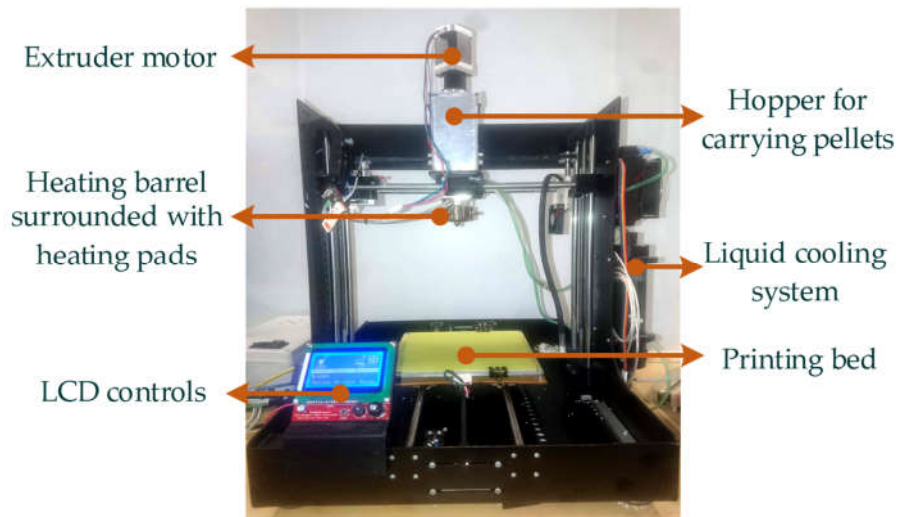

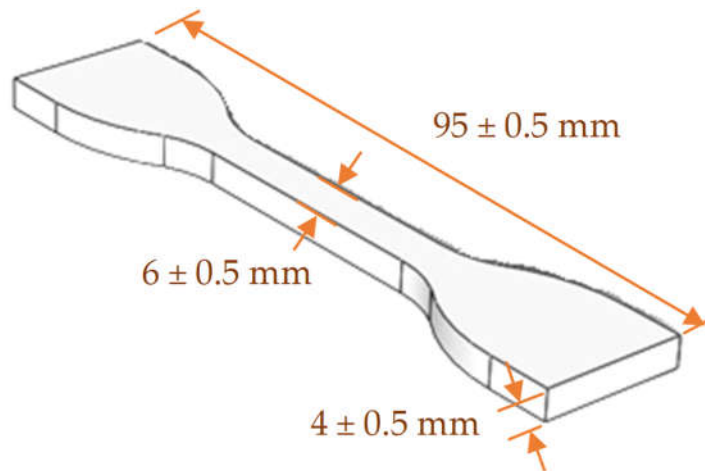**Figure 1.** In-house built pellet 3D printer [23].

Figure 2. ASTM D638 Type IV specimen dimensions.

　　Most of the 3D printing parameters were selected based on the optimal or highest mechanical properties reported in literature. For example, the layer thickness of 0.2 mm was reported with optimal tensile strength [12,24,26]. Similarly, raster width was also based on optimal results reported in literature [12,24,26]. The raster angle of 45°/−45° was also used in various references for achieving optimal mechanical strength [26]. The multiplier was managed as per requirement for both blends. The multiplier is the amount of material extruded out in a unit time (minute). In this regard, the various trials were printed to find the optimal multiplier that is able to achieve extrusion of each bead.

Table 3. Parameters for screw extrusion 3d printing.

Parameters	Values
Layer thickness	0.2 mm [12,24,26]
Raster width	0.2 mm [12,24,26]
Raster angle	45°/−45° [26]
Infill density	100% [12,24]
Multiplier	15
Nozzle diameter	0.4 mm [26]

2.5. Mechanical Testing

　　The tensile testing was performed at an extension rate of 5 mm/min. Instron 5967 was used with a load cell of 30 kN with a 25.4 mm extensometer. The average of tensile of multiple samples were used as final values.

2.6. Fourier Transform Infrared Spectroscopy (FTIR)

　　FTIR analysis was used to investigate the nature of intermolecular interactions between ABS, HDPE, PP, and PE-g-MAH. The variations in intensities and shifts of wavelengths for different chemical groups were noted as intermolecular interactions. The testing was performed on Thermo electron Nicolet 8700. The testing includes 32 scans for each sample that covers a wavelength range of 400 to 4000 cm^{-1}. The transmittance mode was selected for analysing all spectrums.

2.7. Thermogravimetric Analysis (TGA)

　　The TGA analysis was performed to investigate the nature of intermolecular interactions (physical grafting or chemical grafting). The analysis is performed on STA 449 F1

Jupiter by NETZSCH in a range of 25 °C to 550 °C. The rate of analysis was set at 10 °C/min using a nitrogen purging of 50 mL/min.

3. Results

3.1. Polymer Melt Blending

The aim of this research is to achieve successful 3D printing rather than optimizing the blend composition. The composition of HDPE and PP is a decisive factor to achieve successful 3D printing. In this regard, first blend was prepared in single screw extruder with a composition of 48% by weight of each HDPE and PP in 48% of ABS. The PE-g-MAH is added in 4% by weight [27,28]. The 3D printing of both blends with 48:48:4 composition was not successful. The 3D prints were noted with high die swelling and warpage. The reason for high die swelling is the high composition of MAH [29], and the warpage is caused due to the high composition of HDPE and PP [30,31]. Therefore, the second blend composition was prepared with decreased contents of PP, HDPE, and PE-g-MAH. Each HDPE and PP were added in 7.5 weight percentage with 92.5% ABS with 0.5% of PE-g-MAH [32]. The second composition of for both ABS:HDPE:PE-g-MAH and ABS:PP:PE-g-MAH were successfully 3D-printed with no warpage or die swelling. Therefore, the third blend composition was not prepared.

3.2. Tensile Testing

The results of ANOVA analysis for tensile strength are provided in Figure 3 and Table 4. The analysis shows that all variables are insignificant. The insignificance of all variables shows that all three variables (build surface temperature, printing temperature, and polymer additives) have similar values of tensile strength as presented in Table 4. The highest tensile strength for ABS:HDPE:PE-g-MAH and ABS:PP:PE-g-MAH are 30.89 MPa and 30.3 MPa, respectively. The highest tensile strength for ABS:HDPE:PE-g-MAH is noted at combination of 190 °C and 70 °C. On the other hand, the highest tensile strength for ABS:PP:PE-g-MAH is obtained at combination of 190 °C and 50 °C.

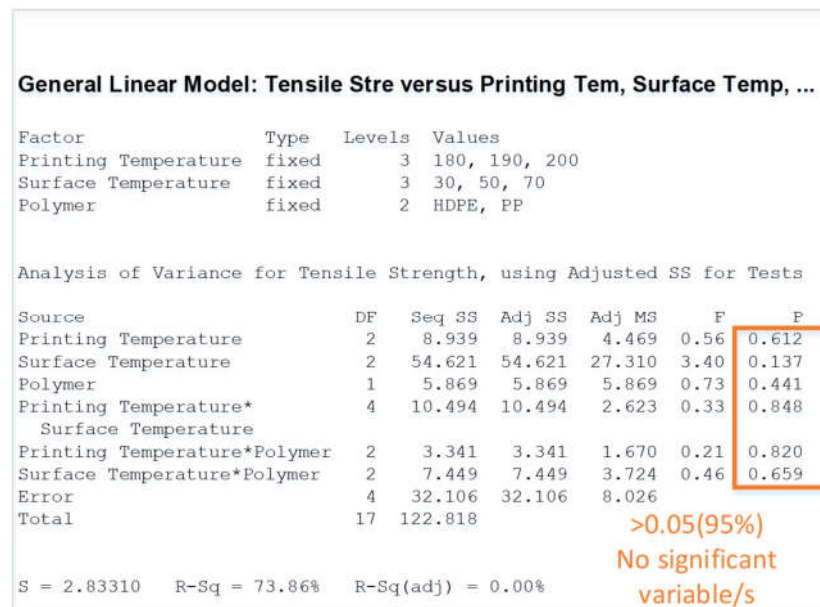The reasons for insignificance are discussed in discussion.

General Linear Model: Tensile Stre versus Printing Tem, Surface Temp, ...

Factor	Type	Levels	Values
Printing Temperature	fixed	3	180, 190, 200
Surface Temperature	fixed	3	30, 50, 70
Polymer	fixed	2	HDPE, PP

Analysis of Variance for Tensile Strength, using Adjusted SS for Tests

Source	DF	Seq SS	Adj SS	Adj MS	F	P
Printing Temperature	2	8.939	8.939	4.469	0.56	0.612
Surface Temperature	2	54.621	54.621	27.310	3.40	0.137
Polymer	1	5.869	5.869	5.869	0.73	0.441
Printing Temperature* Surface Temperature	4	10.494	10.494	2.623	0.33	0.848
Printing Temperature*Polymer	2	3.341	3.341	1.670	0.21	0.820
Surface Temperature*Polymer	2	7.449	7.449	3.724	0.46	0.659
Error	4	32.106	32.106	8.026		
Total	17	122.818				

$>0.05(95\%)$
No significant variable/s

S = 2.83310   R-Sq = 73.86%   R-Sq(adj) = 0.00%

Figure 3. ANOVA analysis.

<p align="center">**Table 4.** Tensile strength for ANOVA DoE.</p>

StdOrder	RunOrder	PtType	Blocks	Printing Temperature (C°)	Surface Temperature (C°)	Polymer	Tensile Strength (MPa)
3	1	1	1	180	50	HDPE	25.533
10	2	1	1	190	50	PP	30.3
2	3	1	1	180	30	PP	28.5
15	4	1	1	200	50	HDPE	24.456
6	5	1	1	180	70	PP	28.3
17	6	1	1	200	70	HDPE	30.592
9	7	1	1	190	50	HDPE	23.395
14	8	1	1	200	30	PP	25.1
5	9	1	1	180	70	HDPE	27.714
16	10	1	1	200	50	PP	28.9
12	11	1	1	190	70	PP	30.5
7	12	1	1	190	30	HDPE	25.04
1	13	1	1	180	30	HDPE	24.72
13	14	1	1	200	30	HDPE	28.084
4	15	1	1	180	50	PP	23.1
8	16	1	1	190	30	PP	25.6
11	17	1	1	190	70	HDPE	30.895
18	18	1	1	200	70	PP	30.4

4. Discussion

4.1. ANOVA Analysis

The ANOVA analysis in Figure 3 presents insignificance for all variables. The in-depth analysis shows that the tensile strength for HDPE-based combinations have a standard deviation of 2.6 MPa as compared to 2.5 MPa of PP-based combinations. The minimum difference of tensile values concludes the overall variations negligible. Therefore, the ANOVA analysis merely based on confidence level (95%) is not a true representative to explain the comparison between HDPE and PP based ABS blends in this research.

In this regard, the individual effects of each variable on tensile strength reveals true behaviour as noted in "main effects plot" (Figure 4). The "main effects plot" shows the increase of tensile strength with increase of printing temperature, i.e., from ≈26 MPa to ≈28 MPa. Similarly, the increase in surface (bed) temperature results in increase of tensile strength, i.e., from ≈26 MPa to ≈30 MPa (Figure 4). Moreover, the two polymer additives (HDPE and PP) also report increase for PP based ABS blend (≈28 MPa) as compared to HDPE based ABS blends (≈26.5 MPa). This shows that the impact of PP is more as compared to HDPE on ABS blends.
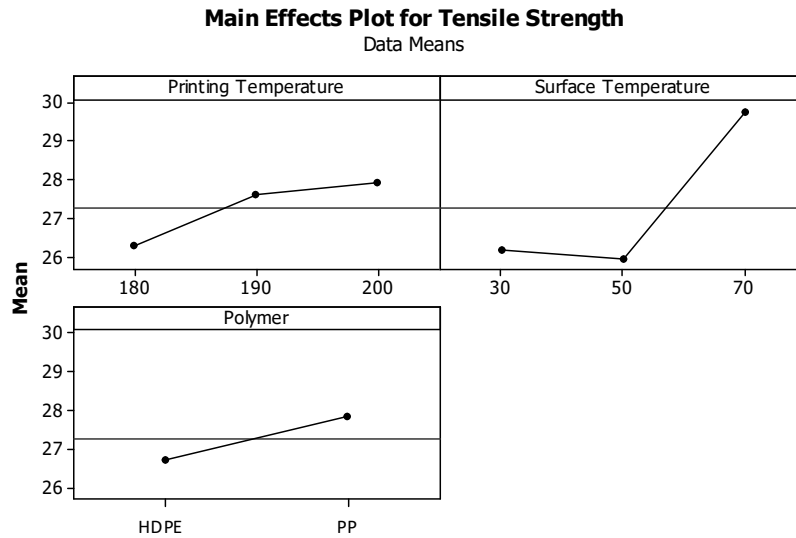
Main Effects Plot for Tensile Strength
Data Means

Figure 4. Mian effects plot for tensile strength.

Additionally, the binary interactions in "interaction plot" also describe the variations due to the polymer additives and in-process temperatures (Figure 5). For example, the binary interaction of printing temperature and polymer additives in ABS blends provides visible increase in tensile strength. The Figure 5 shows the binary increase of tensile strength for PP with increase of printing temperature. Similarly, the surface (bed) temperature also presents highest tensile strength with increase of bed temperature to 70 °C.

Interaction Plot for Tensile Strength
Data Means
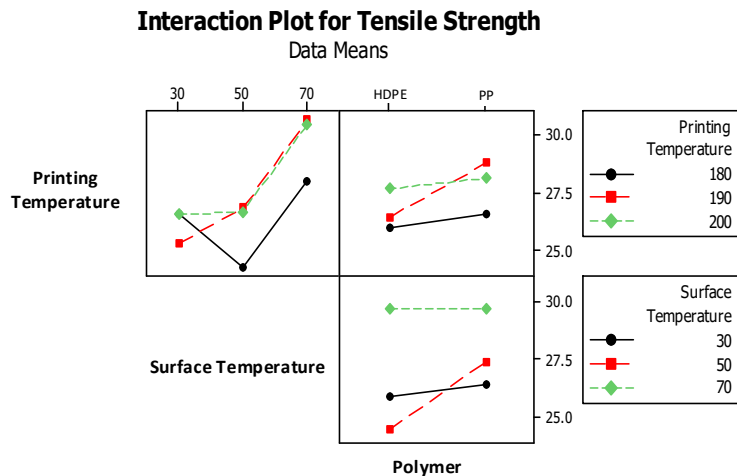
Figure 5. Interaction plot for tensile strength.

One of the probable reasons for insignificance of three variables (printing temperature, bed temperature, and polymers) is the similar chemical nature of blends that results in similar tensile values. Therefore, the chemical analysis in form of FTIR and TGA are provided in the subsequent discussion.

4.2. Intermolecular Interactions Using FTIR

FTIR analysis for ABS, HDPE, PP, and PE-g-MAH are given in Figure 6. The FTIR spectrum of High-density polyethylene (HDPE) is confirmed with C-H groups [33] at 2912.5 cm^{-1} and 2846 cm^{-1}. For PE-g-MAH, the polyethylene [34] is detected at 2915 cm^{-1} and 2848 cm^{-1}. The maleic anhydride (MAH) is detected at 1715 cm^{-1} [34]. Polypropylene

(PP) is confirmed with C-H peaks at 2949.6 cm^{-1}, 2916.8 cm^{-1}, and 2837 cm^{-1}. Acrylonitrile butadiene styrene (ABS) is validated with peaks associated with acrylonitrile at 2238 cm^{-1}, butadiene at 1638 cm^{-1}, styrene at 1494 cm^{-1} [35].

The analysis of ABS blend with HDPE shows visible variations as shown in Figure 6. The overall spectrum of ABS:HDPE:PE-g-MAH is similar to neat ABS. However, the differences are in form of shifts in wavelengths and decrease or increase of intensities. For example, C-H bond of hydrocarbons shifts from 2919 cm^{-1} to 2917.3 cm^{-1} and 2847 cm^{-1} to 2848 cm^{-1}. Acrylonitrile shifts from 2238 cm^{-1} to 2239 cm^{-1}. Styrene shifts from 1494 cm^{-1} to 1493 cm^{-1}. Apart from minor changes, couple of major changes includes the absence of nonsaturated hydrocarbon bond and butadiene peak [34,35] in ABS blend. The shifts in wavelengths and absence of peak shows evidence of intermolecular interactions in ABS:HDPE:PE-g-MAH blend.

The analysis of ABS blend with PP also shows prominent variations in Figure 6. The minor shift in following groups is noted: nonsaturated hydrocarbons from 3028 cm^{-1} to 3027 cm^{-1}, saturated hydrocarbons from 2919 cm^{-1} to 2917.3 cm^{-1}, and 2847 cm^{-1} to 2849 cm^{-1}. Furthermore, the intensities of all chemical groups are changed as compared to that of neat ABS. therefore, the variations in wavelengths and intensities shows the intermolecular interactions.

Figure 6 shows that the intensity for C-H at 2849.3 cm^{-1} and styrene at 1494 cm^{-1} is comparatively lower for PP-based blend. The low intensities in ABS:PP:PE-g-MAH are due to the restricted vibrations of corresponding groups. Therefore, it identifies the higher impact of PP as compared to HDPE. The high restricted vibrations identified with low intensities may be the reason for high mechanical strength for ABS:PP:PE-g-MAH as compared to ABS:HDPE:PE-g-MAH.

However, the information regarding stability to thermal degradation can validate the low intensities in FTIR as a reason for high mechanical strength.
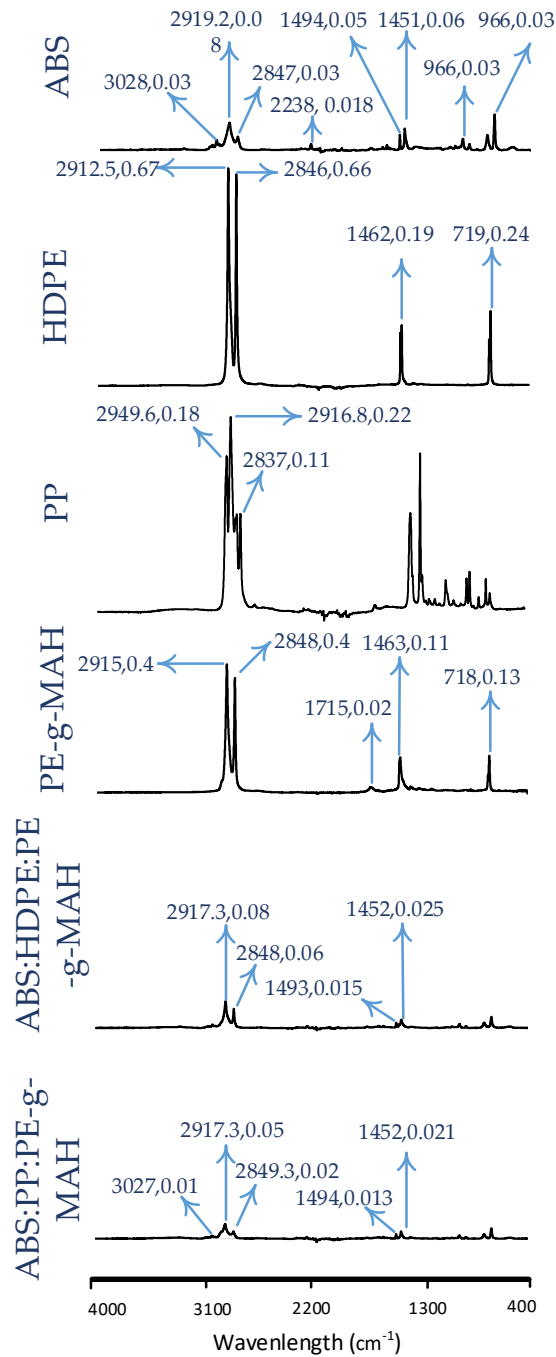
Figure 6. FTIR analysis for different polymers and 3D-printed blends.

4.3. Thermogravimetric Analysis

The TGA thermographs are provided in Figure 7. The TGA analysis shows the differences in the temperatures for onset of degradation in both blends. The onset temperature for ABS:PP:PE-g-MAH is comparatively high for to ABS:PP:PE-g-MAH, i.e., ≈406 °C as compared to 404 °C of ABS:HDPE:PE-g-MAH. The difference is minor that validates the similar FTIR graphs for both blends. Similarly, the minor differences in intensities are also justified in form of minor difference of onset temperatures but with ABS:PP:PE-g-MAH with higher numbers. This proves the reason for comparatively high tensile strength of ABS:PP:PE-g-MAH as compared to that of ABS:HDPE:PE-g-MAH.
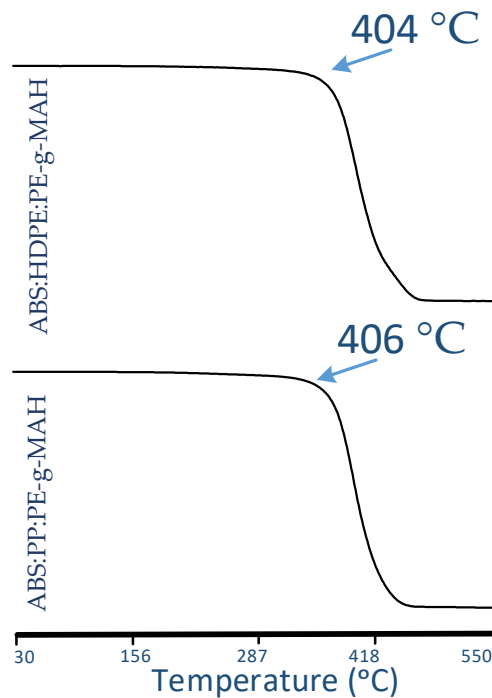
Figure 7. TGA analysis for blends.

5. Conclusions

This research presents a novel statistical and thermochemical comparison for two blends of ABS, i.e., ABS:HDPE:PE-g-MAH and ABS:PP:PE-g-MAH. The effects of two temperature based in-process variables (printing and build surface temperatures) and one polymer-based variable (HDPE and PP) on tensile strength are statistically presented. The research concludes notable effects of polymer additives and in-process variables. However, the ANOVA analysis reveals all variables similar enough to be insignificant with confidence level of greater than 5% (0.05).

Apart from insignificance of three variables (build surface temperature, printing temperature, and polymer additives), various important results are noteworthy. For example, the tensile strength for both ABS:HDPE:PE-g-MAH and ABS:PP:PE-g-MAH is noted with increase of bed and build surface temperatures. In ANOVA analysis, the ABS blend with PP (ABS:PP:PE-g-MAH) achieves higher tensile strength as compared to that of the ABS:HDPE:PE-g-MAH. The reason for high strength of ABS:PP:PE-g-MAH is found in FTIR analysis. FTIR analysis reveals the low restricted vibrations as a reason for high strength of ABS:PP:PE-g-MAH. The restricted vibrations are observed in form of low intensities. TGA analysis validates the low intensities of FTIR analysis through high onset temperatures.

References

1. Peterson, A.M. Review of acrylonitrile butadiene styrene in fused filament fabrication: A plastics engineering-focused perspective. *Addit. Manuf.* **2019**, *27*, 363–371, doi:10.1016/j.addma.2019.03.030.
2. Debbah, I.; Krache, R.; Aranburu, N.; Etxeberria, A.; Pérez, E.; Benavente, R. Influence of ABS Type and Compatibilizer on the Thermal and Mechanical Properties of PC/ABS Blends. *Int. Polym. Process.* **2020**, *35*, 83–94, doi:10.3139/217.3858.
3. Lee, C.; Padzil, F.; Lee, S.; Ainun, Z.; Abdullah, L. Potential for Natural Fiber Reinforcement in PLA Polymer Filaments for Fused Deposition Modeling (FDM) Additive Manufacturing: A Review. *Polymer* **2021**, *13*, 1407, doi:10.3390/polym13091407.
4. Awasthi, P.; Banerjee, S.S. Fused deposition modelling of thermoplastic elastomeric materials: Challenges and opportunities. *Addit. Manuf.* **2021**, *46*, 102177, doi:10.1016/j.addma.2021.102177.
5. Olivera, S.; Muralidhara, H.B.; Venkatesh, K.; Gopalakrishna, K.; Vivek, C.S. Plating on acrylonitrile–butadiene–styrene (ABS) plastic: A review. *J. Mater. Sci.* **2016**, *51*, 3657–3674.
6. Milionis, A.; Languasco, J.; Loth, E.; Bayer, I. Analysis of wear abrasion resistance of superhydrophobic acrylonitrile butadiene styrene rubber (ABS) nanocomposites. *Chem. Eng. J.* **2015**, *281*, 730–738, doi:10.1016/j.cej.2015.06.086.
7. Kulich, D.M.; Gaggar, S.K.; Lowry, V.; Stepien, R. Acrylonitrile-Butadiene-Styrene Polymers. *Encycl. Polym. Sci. Technol.* **2001**, *1*, doi:10.1002/0471440264.pst011.
8. Arostegui, A.; Sarrionandia, M.; Aurrekoetxea, J.; Urrutibeascoa, I. Effect of dissolution-based recycling on the degradation and the mechanical properties of acrylonitrile–butadiene–styrene copolymer. *Polym. Degrad. Stab.* **2006**, *91*, 2768–2774, doi:10.1016/j.polymdegradstab.2006.03.019.
9. Li, Y.; Shimizu, H. Improvement in toughness of poly(l-lactide) (PLLA) through reactive blending with acrylonitrile–butadiene–styrene copolymer (ABS): Morphology and properties. *Eur. Polym. J.* **2009**, *45*, 738–746, doi:10.1016/j.eurpolymj.2008.12.010.
10. Xu, X.; Wang, R.; Tan, Z.; Yang, H.; Zhang, M.; Zhang, H. Effects of polybutadiene-g-SAN impact modifiers on the morphology and mechanical behaviors of ABS blends. *Eur. Polym. J.* **2005**, *41*, 1919–1926, doi:10.1016/j.eurpolymj.2005.02.025.
11. Tiganis, B.; Burn, L.; Davis, P.; Hill, A. Thermal degradation of acrylonitrile–butadiene–styrene (ABS) blends. *Polym. Degrad. Stab.* **2002**, *76*, 425–434.
12. Harris, M.; Potgieter, J.; Mohsin, H.; Chen, J.Q.; Ray, S.; Arif, K.M. Partial Polymer Blend for Fused Filament Fabrication with High Thermal Stability. *Polymer* **2021**, *13*, 3353, doi:10.3390/polym13193353.
13. Meincke, O.; Kaempfer, D.; Weickmann, H.; Friedrich, C.; Vathauer, M.; Warth, H. Mechanical properties and electrical conductivity of carbon-nanotube filled polyamide-6 and its blends with acrylonitrile/butadiene/styrene. *Polymer* **2004**, *45*, 739–748, doi:10.1016/j.polymer.2003.12.013.
14. Canto, L.B.; Mantovani, G.L.; Covas, J.A.; Hage, E.; Pessan, L.A. Phase morphology development during processing of compatibilized and uncompatibilized PBT/ABS blends. *J. Appl. Polym. Sci.* **2007**, *104*, 102–110, doi:10.1002/app.24518.
15. Torrado, A.R.; Shemelya, C.M.; English, J.D.; Lin, Y.; Wicker, R.B.; Roberson, D.A. Characterizing the effect of additives to ABS on the mechanical property anisotropy of specimens fabricated by material extrusion 3D printing. *Addit. Manuf.* **2015**, *6*, 16–29, doi:10.1016/j.addma.2015.02.001.
16. Rocha-Gutierrez, C.; Perez, A.R.T.; Roberson, D.A.; Shemelya, C.M.; MacDonald, E.; Wicker, R.B. Novel ABS-based binary and ternary polymer blends for material extrusion 3D printing. *J. Mater. Res.* **2014**, *29*, 1859–1866, doi:10.1557/jmr.2014.158.
17. Chen, S.; Lu, J.; Feng, J. 3D-Printable ABS Blends with Improved Scratch Resistance and Balanced Mechanical Performance. *Ind. Eng. Chem. Res.* **2018**, *57*, 3923–3931, doi:10.1021/acs.iecr.7b05074.
18. Harris, M.; Potgieter, J.; Ray, S.; Archer, R.; Arif, K.M. Acrylonitrile Butadiene Styrene and Polypropylene Blend with Enhanced Thermal and Mechanical Properties for Fused Filament Fabrication. *Materials* **2019**, *12*, 4167, doi:10.3390/ma12244167.
19. Harris, M.; Potgieter, J.; Ray, S.; Archer, R.; Arif, K.M. Preparation and characterization of thermally stable ABS/HDPE blend for fused filament fabrication. *Mater. Manuf. Process.* **2020**, *35*, 230–240, doi:10.1080/10426914.2019.1692355.
20. Rizvi, R.; Cochrane, B.; Naguib, H.; Lee, P.C. Fabrication and characterization of melt-blended polylactide-chitin composites and their foams. *J. Cell. Plast.* **2011**, *47*, 283–300, doi:10.1177/0021955x11402549.
21. Hoang, V.T.; Tao, Q.B.; Truong-Le, B.-T.; Tran, M.S.; Luu, D.B. Experimental study on mechanical behaviors of injection molded PC/PMMA blends. *J. Mech. Sci. Technol.* **2021**, *35*, 3959–3966, doi:10.1007/s12206-021-0809-4.
22. Van Thanh, H.; Chen, C.C.A.; Kuo, C.H. Injection Molding of PC/PMMA Blend for Fabricate of the Secondary Optical Elements of LED Illumination. *Adv. Mater. Res.* **2012**, *579*, 134–141, doi:10.4028/www.scientific.net/amr.579.134.
23. Whyman, S.; Arif, K.M.; Potgieter, J. Design and development of an extrusion system for 3D printing biopolymer pellets. *Int. J. Adv. Manuf. Technol.* **2018**, *96*, 3417–3428, doi:10.1007/s00170-018-1843-y.
24. Harris, M.; Potgieter, J.; Ray, S.; Archer, R.; Arif, K.M. Polylactic acid and high-density polyethylene blend: Characterization and application in additive manufacturing. *J. Appl. Polym. Sci.* **2020**, *137*, 49602, doi:10.1002/app.49602.

25. ASTM International. ASTM D638-14, Standard Test Method for Tensile Properties of Plastics. ASTM International, 2015. Available online: https://en.wikipedia.org/wiki/List_of_ASTM_International_standards (accessed on 21 November 2021).

26. Harris, M.; Potgieter, J.; Archer, R.; Arif, K.M. Effect of Material and Process Specific Factors on the Strength of Printed Parts in Fused Filament Fabrication: A Review of Recent Developments. *Materials* **2019**, *12*, 1664, doi:10.3390/ma12101664.

27. Hwang, K.-J.; Park, J.-W.; Kim, I.; Ha, C.-S.; Kim, G.-H. Effect of a compatibilizer on the microstructure and properties of partially biodegradable LDPE/aliphatic polyester/organoclay nanocomposites. *Macromol. Res.* **2006**, *14*, 179–186, doi:10.1007/bf03218506.

28. Yu, G.; Ji, J.; Zhu, H.; Shen, J. Poly (D, L-lactic acid)-block-(ligand-tethered poly (ethylene glycol)) copolymers as surface additives for promoting chondrocyte attachment and growth. *J. Biomed. Mater. Res. Part B Appl. Biomater. Off. J. Soc. Biomater. Jpn. Soc. Biomater. Aust. Soc. Biomater. Korean Soc. Biomater.* **2006**, *76*, 64–75.

29. Zhang, L.; Lv, S.; Sun, C.; Wan, L.; Tan, H.; Zhang, Y. Effect of MAH-g-PLA on the Properties of Wood Fiber/Polylactic Acid Composites. *Polymer* **2017**, *9*, 591, doi:10.3390/polym9110591.

30. Dong, M.; Zhang, S.; Gao, D.; Chou, B. The study on polypropylene applied in fused deposition modelling. *AIP Conf. Proc.* **2019**, *2065*, 030059, doi:10.1063/1.5088317.

31. Carneiro, O.S.; Silva, A.F.; Gomes, R. Fused deposition modelling with polypropylene. *Mater. Des.* **2015**, *83*, 768–776, doi:10.1016/j.matdes.2015.06.053.

32. Supri, A.G.; Ismail, H.; Shuhadah, S. Effect of Polyethylene-Grafted Maleic Anhydride (PE-g-MAH) on Properties of Low Density Polyethylene/Eggshell Powder (LDPE/ESP) Composites. *Polym. Technol. Eng.* **2010**, *49*, 347–353, doi:10.1080/03602550903414035.

33. Da Silva, D.J.; Wiebeck, H. CARS-PLS regression and ATR-FTIR spectroscopy for eco-friendly and fast composition analyses of LDPE/HDPE blends. *J. Polym. Res.* **2018**, *25*, 112.

34. Birnin-Yauri, A.U.; Ibrahim, N.A.; Zainuddin, N.; Abdan, K.; Then, Y.Y.; Chieng, B.W. Effect of Maleic Anhydride-Modified Poly(lactic acid) on the Properties of Its Hybrid Fiber Biocomposites. *Polymer* **2017**, *9*, 165, doi:10.3390/polym9050165.

35. Li, J.; Chen, F.; Yang, L.; Jiang, L.; Dan, Y. FTIR analysis on aging characteristics of ABS/PC blend under UV-irradiation in air. *Spectrochim. Acta Part A Mol. Biomol. Spectrosc.* **2017**, *184*, 361–367, doi:10.1016/j.saa.2017.04.075.